

# Ballistic Properties of Hybrid Thermoplastic Composites with Silica Nanoparticles

Vera Obradović, Dušica B. Stojanović, PhD, Radmila Jančić – Heinemann, PhD, Irena Živković, PhD, Vesna Radojević, PhD, Petar S. Uskoković, PhD, Radoslav Aleksić, PhD

University of Belgrade, Faculty of Technology and Metallurgy, Belgrade, SERBIA

Correspondence to:

Vera Obradović email: [yobradovic@tmf.bg.ac.rs](mailto:yobradovic@tmf.bg.ac.rs)

## ABSTRACT

Multi-axial aramid fabrics have a wide range of applications in the construction of composite structures for body armor. Nanoparticles, which include nanosilica, are one of the most common nanofillers for these structures. The particles of nanosilica possess nanometer dimensions with high specific surface area. Silane coupling agents are mostly used for modifying nanosilica surface in order to prevent silica agglomeration. Incorporation of nanosilica treated with silane adhesion promoter, in the matrix part of the hybrid composite form, leads to increased resistance to the bullet shock impact.

In this study, the resistance to penetration of a shot bullet was tested for four samples of the aramid fabric composite forms. All fabrics were coated with  $\gamma$ -aminopropyl triethoxysilane (AMEO silane)/ethanol solution. Two samples were impregnated with poly (vinyl butyral) (PVB)/ethanol solution, while the other two were impregnated with the same solution, but with the addition of the 30 wt.% AMEO silane modified silica nanoparticles as reinforcement. The samples were both hard and flexible options. The bullet-shooting test was applied to all the composites by two different bullet types. The structural design of the samples improved the ballistic resistance after the bullets were shot. Some ballistic image analyses for print and penetration depth of the samples were performed using Image Pro-Plus software.

## INTRODUCTION

Woven and nonwoven fabrics made of high tenacity fibers are used in ballistic protection, and are characterized by low density, high strength and high energy absorption capability. It is assumed that the ballistic performance of a material depends on its capability to absorb energy, and its efficiency to spread out energy quickly. Tenacity and elongation at

fracture of the fiber are assumed to be the most important properties of the fiber based (textile) armor [1]. It is understood that the main function of the vest is to block the projectile, but also to absorb the shock of the crash. Thus, the second function of modern ballistic protection is to dissipate the kinetic energy of a projectile so that only a fraction of its blow is transmitted to the body [2]. The bullet mass and speed determine its kinetic energy, and higher kinetic energy causes more deformation. When a woven fabric is subjected to ballistic impact, the deformation on the fabric spreads outwards when the bullet speed remains within the limits. The degree of deformation depends on the fabric structure. As the bullet speed exceeds a certain limit, the bullet passes through the fabric. The fabric layers have a limited energy absorption capacity and it is necessary to develop different designs in order to block the bullet when the bullet kinetic energy exceeds the energy absorption limit of the fabric [3, 4]. There are two main categories of the body armor that provide protection from different types of ballistic missiles. One of them is the 'hard body armor', which combines ceramic and composites and is produced to give protection from high-velocity (rifle) bullets, while the other one is the 'soft body armor' which supplies fabrics with protection from low-velocity (hand-gun) bullets. The 'soft body armor' is usually constructed of the multiple layers of the fabric commonly known as the 'ballistic panel', which is injected into a 'carrier' composed of a polyester/cotton or nylon woven fabric and may be inserted into a light-resistant (or water-resistant) cover. The 'soft body armor' worn by police officers is produced to provide protection from stab threats and hand-gun bullets, while the military body armor is designed to bring protection from fragmentation threats, which are the most frequent injuries in modern war fighting [5]. There has been a significant development of new high-performance armor materials for lightweight

body-armor and lightweight vehicle-armor structures. Flexible lightweight materials have been used in the body-armor systems to provide protection against certain types of risks without upsetting human mobility. High-performance polymeric fibers are now the standard in various woven fiber-reinforced body-armor utilization, although, due to their low cost, nylon and E-glass fibers are still in use today [6]. Besides them, R- and S-glass fibers are having increased presence in ballistic products as well [1]. High-performance polymeric fibers used today are characterized by their superior strength, stiffness and ballistic performance. Among these high-performance fibers the most notable are poly-aramids (Kevlar, Twaron, Technora), high performance polyethylene (HPPE) fibers (Dyneema, Spectra), poly-benzobis-oxazole, PBO (Zylon) and poly-pyridobisimi-dazole, PIPD (M5). In tension, these fibers behave as rate independent linear elastic materials, and when tested in transverse compression, can withstand large plastic deformation without a significant loss in their tensile load-carrying capacity [6].

Ceramic has usually been used in body armor due to properties, such as introducing overall flexibility and reducing the weight of the fabric system [7]. The addition of nanoscale ceramic reinforcement to polymer matrices improves the mechanical properties significantly, as compared to the pure matrix material in the body armor [8]. Nanosilica is one of the main nanofillers used in polymer composites. Silica nanoparticles are characterized by their high specific surface area. Due to their agglomeration, silane coupling agents are used for modifying nanosilica surface for most applications [9]. The introduction of silane causes better dispersion and deagglomeration of the silica particles, as well as the formation of chemical bonds between them and organic constituents [8].

Modern flexible armor is made mainly from shear thickening fluid (STF)-Kevlar composites, where STF is impregnated into the Kevlar fabrics. STF represents the suspension of about 55 wt.% silica in polyethylene glycol (PEG) [10], or the product of dispersing 52-57% vol. colloidal silica particles in 200 Mw PEG [11, 12]. According to these results, the *p*-aramid fabrics in this work have been impregnated with the PVB solution, but with the addition of the 30 wt.% AMEO modified SiO<sub>2</sub> nanoparticles.

In order to increase the impact resistance of aramid fabric composite forms and to stop the bullet penetration, we introduced silane modified nanosilica and fabricated the hybrid composite system *p*-aramid/PVB/AMEO-30 wt.% SiO<sub>2</sub>.

## MATERIALS AND METHODS

Multi-axial aramid fabrics (Martin Ballistic Mat, Ultratex, Serbia) were used with *p*-aramid fiber type Twaron (Teijin Aramid). Polymer powder poly (vinyl butyral) (Mowital B60H, Kuraray Specialities Europe) and absolute ethanol (Zorka Pharma, Šabac, Serbia) were used for preparing the PVB solution (10 wt.%).

The modification of silica nanoparticles (*Figure 1*) with  $\gamma$ -aminopropyl triethoxysilane (AMEO silane) started with adding the silane into 95 wt.% ethanol-5 wt.% water mixture in order to reach a 2 wt.% final AMEO concentration. The process of hydrolysis and silanol formation lasted for about 10 minutes. After the addition of the nanoparticles, the solution was homogenized with a magnetic stirrer for 30 minutes. After three hours of sonication, the solution was centrifuged at a speed of 3000 rpm for 30 minutes. The particles were placed at the bottom of the beaker and the supernatant was decanted. After that, the particles were rinsed with ethanol and dried in an oven at 110 °C [8]. The modified silica nanoparticles with an average particle diameter of about 7 nm (Evonik-Degussa, Aerosil 380) were introduced into the PVB solution. The neat silica nanoparticle has a high specific surface area of 380±30 m<sup>2</sup>/g. First, all the fabrics were coated with AMEO silane/ethanol solution. The impregnated fabrics were then left to stand for about 24 hours for ethanol evaporation. In the next step, two of the fabrics were coated with poly (vinyl butyral) (PVB)/ethanol solution and the other two were coated with the same solution but with the addition of the 30 wt.% AMEO silane modified silica nanoparticles. The impregnated fabrics were then left to stand for 24 hours whereby the ethanol evaporated. The processing conditions were the same for all the impregnated fabrics. The hard hybrid laminated composite samples were hot-pressed using N 840 D Hix Digital Press (Hix, Corp., USA) at a temperature of 170 °C for 60 minutes under pressure of 4 bar. The fabrics were additionally pressed with P-125 press (170 °C, 8.2 MPa) for 30 minutes. The flexible composite fabrics were stitched together with a lightweight polyester thread (Korteks, Turkey). The two samples were hard pressed with 17 fabric layers, while the flexible samples consisted of 16 fabric layers.

## CHARACTERIZATION

The ballistic impact resistance test was conducted in accordance with the modified ballistic resistance of personal body armor, NIJ standard 0101.04, by using the SABRE ballistics UK Integrated Range Instrument System (IRIS) [13]. This system is an 'all-in-one' control system for weapon and ammunition proofing, research, and range development. In conjunction with a suitably equipped weapon, SABRE Milligan Sky Screens, and an electronic target, all standard measurements can be readily made, recorded, and analyzed.

All samples were tested in accordance with the combined sequences of shooting for the two levels of the ballistic protection - firing sequence for type II and IIIA armor. Two types of bullets were used for the testing: the 357 Magnum FMJ 10.2 g and the 44 Rem. Magnum JHP 15.6 g, with nominal masses of 10.2 g and 15.6 g, respectively. The first four shots (No. 1-4) were fired with the 357 Magnum, and the 44

Rem Magnum was used for the fifth, all being launched at a reference velocity of 436 m/s for each sample as a target. There were fifteen shots in total during the ballistic test: twelve from the 357 Magnum and three from the 44 Rem Magnum.

The composite fabrics were gold-coated and observed under a scanning electron microscope FESEM (JSM 5800). The appropriate SEM images of the *p*-aramid/PVB fabric (*Figure 1a*) and the *p*-aramid/PVB fabric with the AMEO modified silica nanoparticles are depicted in *Figure 1(b-d)*.

The diameter dimensions of the AMEO silane modified nanoparticles were from around 20 nm to 800 nm (*Figure 1c*). The dimensions were analyzed using the software package Image-Pro Plus. It is evident that the AMEO silane modification of the silica nanoparticles contributed to their deagglomeration, due to the small size of some modified nanoparticles.

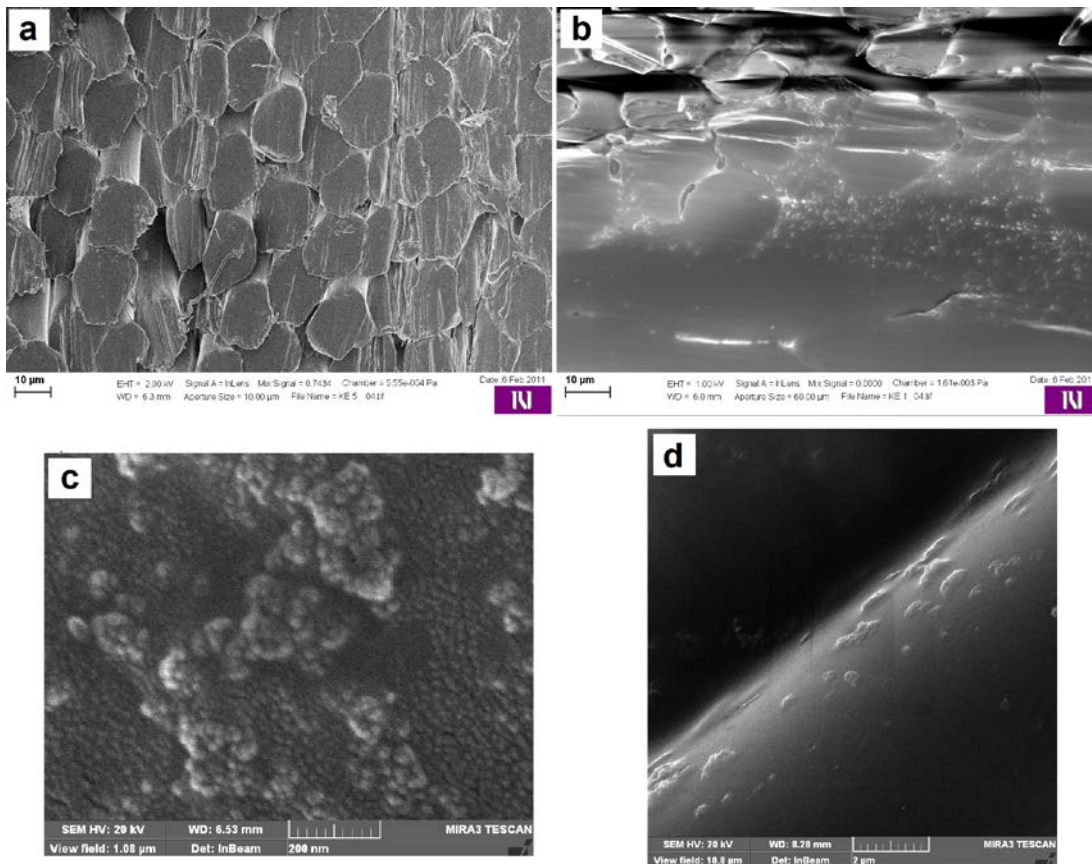


FIGURE 1. SEM image of : a) the *p*-aramid/PVB fabric composite (scale bar 10 μm); b) the *p*-aramid/PVB fabric composite with the 30 wt.% AMEO silane modified silica nanoparticles (scale bar 10 μm); c) the modified silica nanoparticles on the aramid fabric (scale bar 200 nm); d) the modified silica nanoparticles that entered aramid fibers of the fabric (scale bar 2 μm).

The penetration depths of the shots were measured by the digital ruler with nonius PRO-Max (Fowler). The ballistic image analyses for print and penetration depth of the shots were performed using Image Pro-Plus software by converting the images to the grayscale mode, and further subjecting them to bitmap analyses. The produced images were calculated in pixels and converted to millimeters with the purpose of achieving 3D image analysis of the penetration depth. The volumes of the bullet holes represent the sum of the products which are the multiplication of the single units of x and y axes multiplied by the value of the depth at a certain point.

Dynamic mechanical analysis (DMA, Q800 TA Instruments, USA) for the *p*-aramid fabrics was conducted in a dual cantilever mode at a frequency of 1 Hz. The temperature ranged from 20°C to 170 °C with a heating rate of 3 °C/min for the evaluation of the storage modulus ( $E'$ ) and Tan Delta ( $\tan \delta$ ).

## RESULTS AND DISCUSSION

The appropriate modification of silica particles by AMEO silane assumes the hydrolysis of  $\gamma$ -aminopropyl triethoxysilane which provides chemical reaction with the hydroxyl groups at the silica surface. The silanol number  $C_{OH}$  represents the concentration of hydroxyl groups and it is equal to the high value of 3.6 OH/nm<sup>2</sup> in this case [9]. Therefore, the chemical bonds via -OH groups are formed among the AMEO modified silica nanoparticles, AMEO silane impregnated into the fabrics, the polymer matrix PVB and the *p*-aramid fabrics. The mutual bonding enhances the mechanical properties of the composite.

The ballistic results are listed in *Table I*. The samples are denoted as follows: No.1- fabrics with PVB-hard option; No.2- fabrics with PVB and the 30 wt.% AMEO silane modified silica nanoparticles-hard option; No.3- fabrics with PVB-flexible option and No.4- fabrics with PVB and the 30 wt.% AMEO silane modified silica nanoparticles-flexible option. Sample No.1 was eliminated after the first shot because of the complete penetration of bullet No.1. Sample No.3 had no registered velocity for one bullet and therefore the provided number of shots was four instead of five.

TABLE I. Results of the bullet-shooting test.

Shot No.	No. of sample	Type of bullet	Velocity (m/s)	Penetration depth (mm)
1	1	357 Magnum	432.54	complete penetration
2	2	357 Magnum	421.01	11.65
3	2	357 Magnum	431.64	10.3
4	2	357 Magnum	434.62	21.5
5	2	357 Magnum	418.52	15.7
6	2	44 Rem. Magnum	430.2	21.85
7	3	357 Magnum	417.75	7.9
8	3	357 Magnum	417.68	11
9	3	357 Magnum	424.49	11.3
10	3	44 Rem. Magnum	434.32	16.6
11	4	357 Magnum	435.06	11.5
12	4	357 Magnum	432.85	7.2
13	4	357 Magnum	424.31	8
14	4	357 Magnum	429.24	11
15	4	44 Rem. Magnum	429.72	16.5

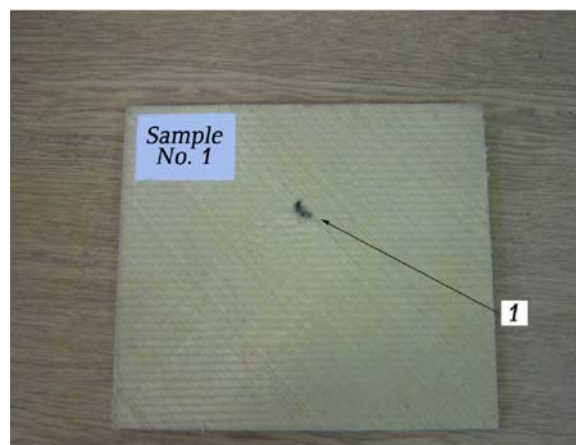


FIGURE 2. Front side of shot sample No.1

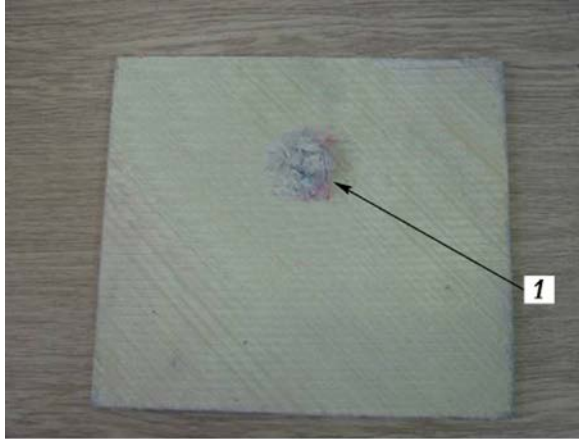


FIGURE 3. Back side of shot sample No.1.

Bullet shooting showed that the composites of *p*-aramid poly (vinyl butyral) could not always act as a full protection against bullets. This is obvious from the complete penetration of bullet No.1 in sample No.1. *Figures 2 and 3* show the entrance and the exit of the bullet in the target.

Unlike the *p*-aramid/PVB composites, both the composites containing SiO<sub>2</sub> nanoparticles stopped all the bullets. The projectiles partially penetrated making the back face deformation of the samples (*Figures 4 and 5*). It can be seen, therefore, that the addition of nanoscale SiO<sub>2</sub> reinforcement led to the improved mechanical properties and ballistic protection of the *p*-aramid/PVB/AMEO-30 wt.% SiO<sub>2</sub> composites.

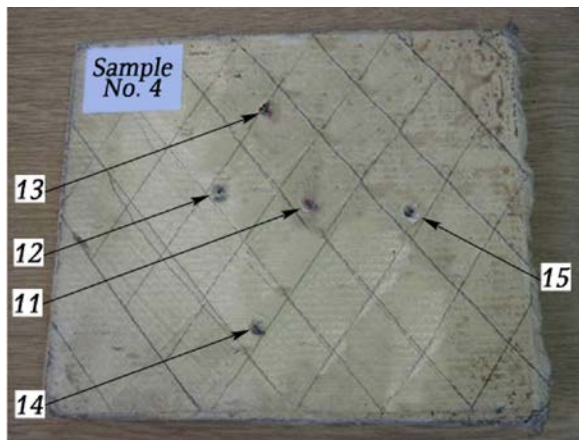


FIGURE 4. Front side of shot sample No.4.

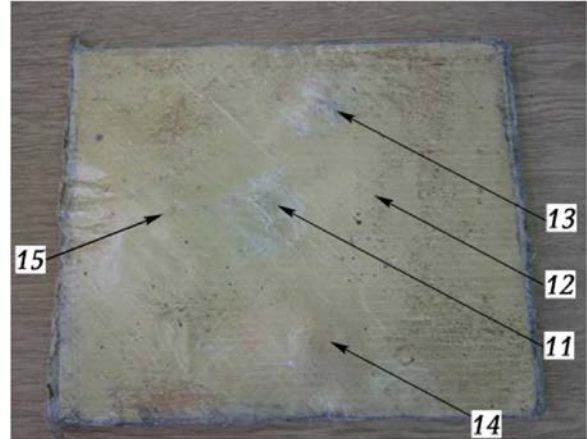


FIGURE 5. Back side of shot sample No.4.

It is evident, from *Table I*, that the 44 Rem. Magnum bullets made a larger penetration depth than the 357 Magnum ones in each sample. This was expected due to the greater mass of the 44 Rem. Magnum bullets. The next stage in the process was the penetration geometry analysis of the three selected shots- No.1, No. 12 and No. 15 (*Figure 6*). The 357 Magnum bullet No.1 completely penetrated the sample No.1, with a thickness of 8.2 mm. The analysis with the millimeter scales of the entrance print of this shot is given in *Figure 7*. An appropriate 3D graph image of the penetration depth is depicted in *Figure 8*.

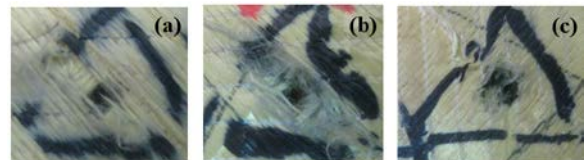


FIGURE 6. Bullet entrances for: (a) shot No.1; (b) shot No.12 and (c) shot No.15.

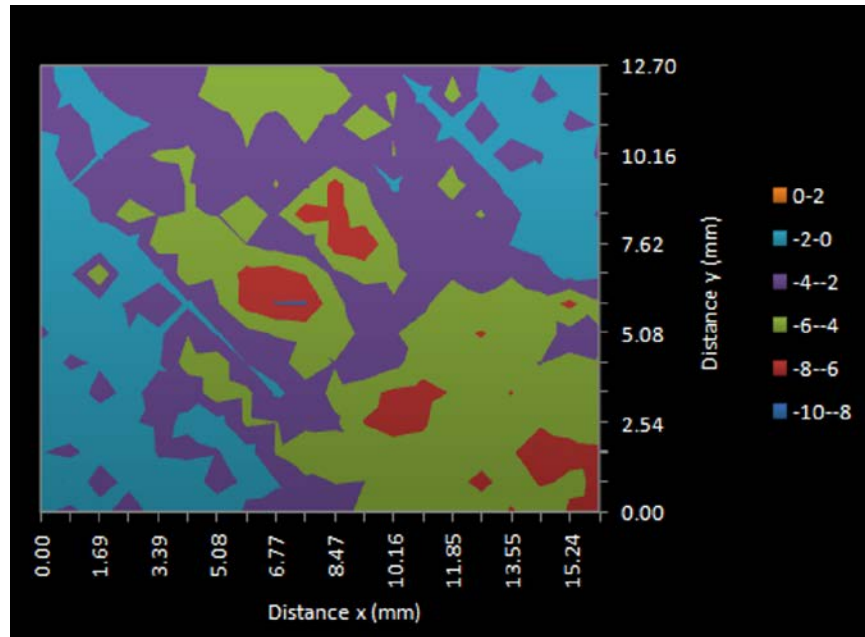


FIGURE 7. Print analysis of shot No.1.

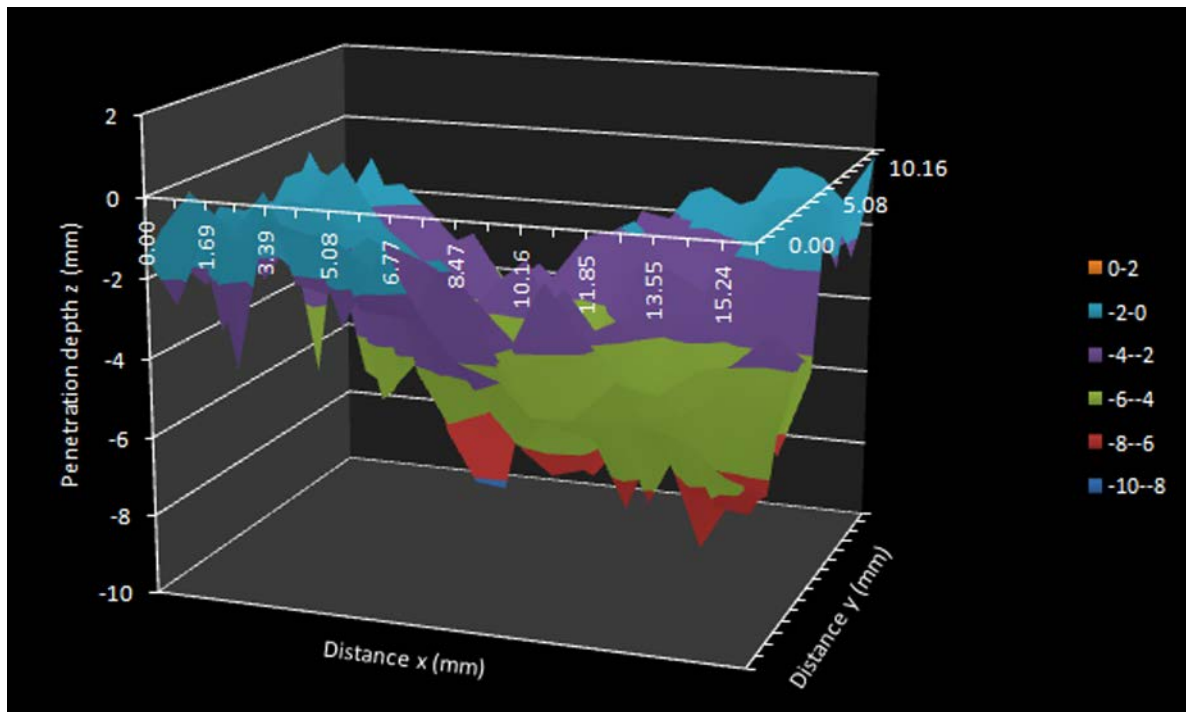


FIGURE 8. Penetration depth analysis of shot No.1

The next two analyzed shots belong to the same sample- No.4 - but they were accomplished with the different projectiles.

The initial thickness of this target was 8.3 mm. Shot No.12 was achieved with the 357 Magnum bullet leading to a penetration depth of 7.2 mm. The adequate graphical analyses are given below (*Figures 9 and 10*).

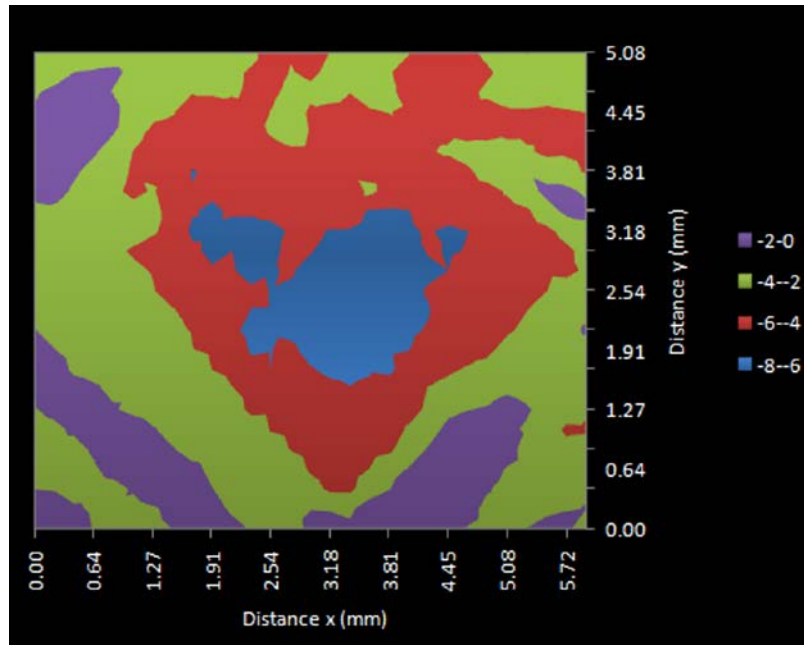


FIGURE 9. Print analysis of shot No.12

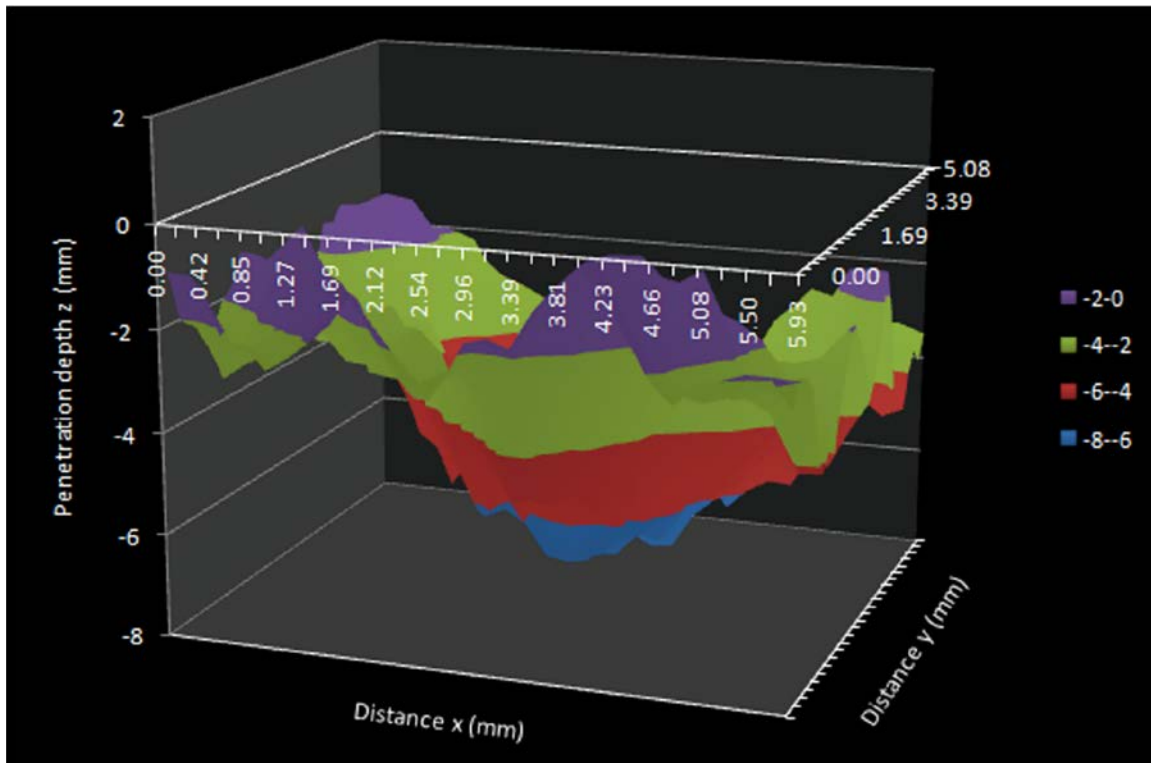


FIGURE 10. Penetration depth analysis of shot No.12.

The result for shot No.15, produced by the 44 Rem. Magnum bullet, showed a larger penetration depth compared to the previous one. The depth was equal to 16.5 mm.

Compared to the initial thickness, this value indicates that the big crater was formed by the back-face deformation due to the partial penetration. The appropriate graphical analyses for this shot are depicted in *Figures 11* and *12*.

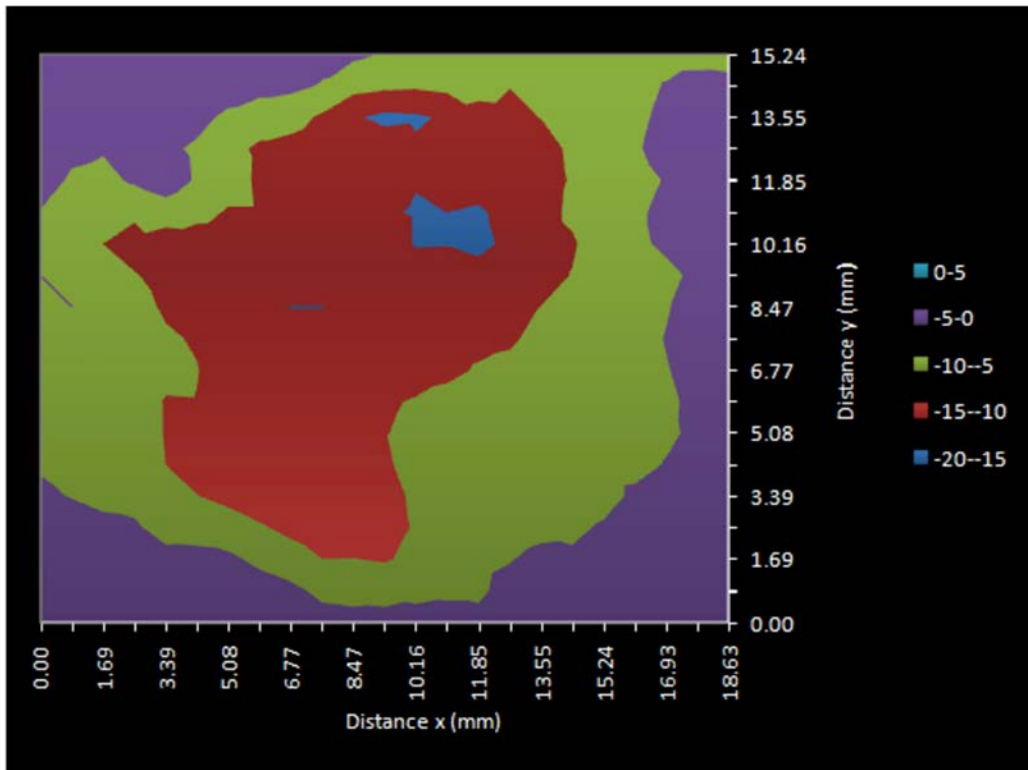


FIGURE 11. Print analysis of shot No.15.

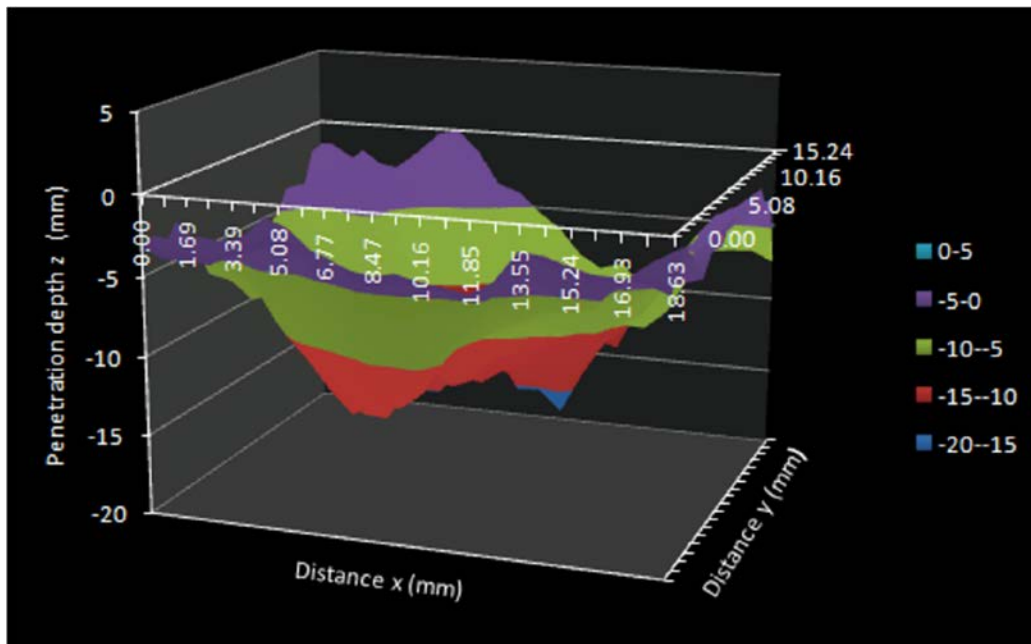


FIGURE 12. Penetration depth analysis of shot No.15.

One pair of the bullet holes (except for the one from the first sample) was selected from each of the samples for comparison of their penetration volumes

(Table II). The first value of the penetration volume in the pair was produced with the 357 Magnum bullet and the second one with the 44 Rem. Magnum bullet.

It is evident that the penetration holes made with the 44 Rem. Magnum bullets had larger volumes along with their greater penetration depths.

TABLE II. Results for the bullet holes.

No. of sample	Shot No.	Penetration depth (mm)	Volume (mm <sup>3</sup> )
1	1	complete penetration	782
2	5	15.7	1973
2	6	21.85	4145
3	7	7.9	1232
3	10	16.6	2380
4	12	7.2	1010
4	15	16.5	2381

### Hard and Flexible Option Comparison

DMA analysis is a thermo-mechanical analysis technique for measuring the viscoelastic properties of materials under periodic sinusoidal stress deformation. The strength value (stress/strain ratio) is in the form of complex modulus  $E^*$  which can be divided into two parts: the elastic part ( $E'$  - storage modulus) and the viscous part ( $E''$  - loss modulus). Tan Delta ( $\tan \delta$ ) is a parameter which provides information on the ratio between  $E'$  and  $E''$  and shows the loss of energy. The above mentioned values can be calculated as follows (Eq. (1), (2), (3), (4)):

$$E^* = E' + iE'' \quad (1)$$

$$E' = |E^*| \cos \delta \quad (2)$$

$$E'' = |E^*| \sin \delta \quad (3)$$

$$\tan \delta = \frac{E''}{E'} \quad (4)$$

The complex modulus  $E^*$  is calculated according to the measured data and the sample geometry for a dual cantilever mode (Eq. (5)):

$$E^*_{dual-cantilever} = \frac{l^3}{16 \cdot b \cdot h^3} \cdot \frac{F}{A} \quad (5)$$

where are:  $l$  – the length of the sample,  $b$  – the width of the sample,  $h$  – the thickness of the sample,  $F$  – the force, and  $A$  – the deflection [14].

The temperature dependences of the storage modulus for sample No.2 (the  $p$ -aramid fabrics with PVB and the 30 wt.% AMEO silane modified silica nanoparticles-hard option) and sample No.4 (the  $p$ -aramid fabrics with PVB and the 30 wt. % AMEO silane modified silica nanoparticles-flexible option) after shooting are depicted in Figure 13. Sample No.2-hard option - displayed a lower value of the storage modulus (368.4 MPa) compared to sample No.4 (the flexible option-769.3 MPa), which indicates that a process of delamination occurred in the hard sample.  $\tan \delta$  of the same samples (Figure 14) shows that sample No.2 had a lower value compared to sample No.4, because of the weak bonds among PVB,  $p$ -aramid and  $\text{SiO}_2$  nanoparticles. With the glass transition temperature of  $T_{g,1} = 68.94 \text{ }^\circ\text{C}$  which originates in PVB, the hard sample exhibited better thermo-mechanical properties than the flexible one ( $T_{g,1} = 64.77 \text{ }^\circ\text{C}$ ), due to the compression treatment in the hard option. The peak belonging to sample No.4 corresponds to the value of  $T_{g,2} = 154.76 \text{ }^\circ\text{C}$ , which is the glass transition temperature of the polyester thread bonded with  $p$ -aramid fabrics.

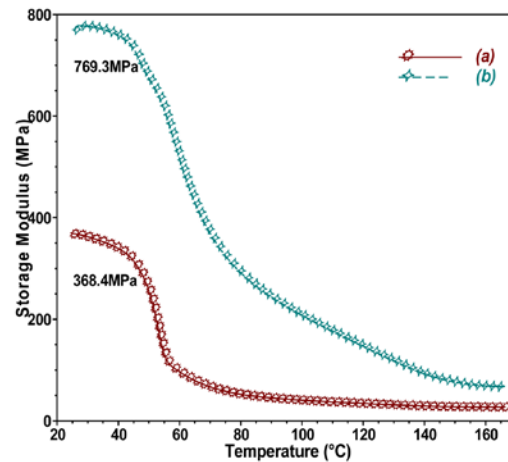


FIGURE 13. Storage modulus of samples: (a) No.2 and (b) No.4

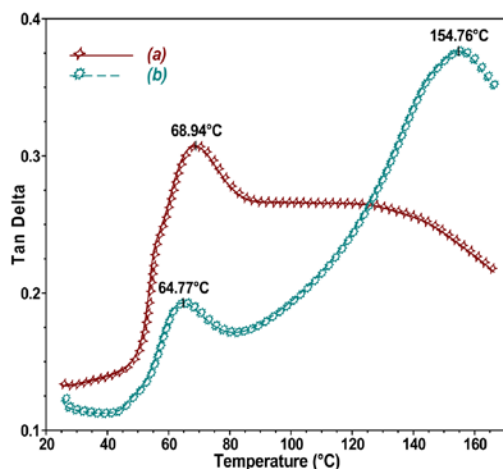


FIGURE 14. Tan Delta ( $\tan \delta$ ) of samples: (a) No.2 and (b) No. 4.

## CONCLUSION

The introduction of the AMEO silane modified silica nanoparticles to the composite of *p*-aramid/poly (vinyl butyral) contributed to the significant improvement in the mechanical properties, producing hybrid ballistic system of higher protection.

After the ballistic test, the flexible option samples yielded better mechanical properties compared to those of the hard option samples.

The storage modulus value of the flexible option sample was more than 100% greater compared to the value of the hard option sample.

## ACKNOWLEDGEMENTS

The authors wish to acknowledge the financial support from the Ministry of Education, Science and Technological Development of the Republic of Serbia through Projects Nos. TR 34011 and III 45019.

## REFERENCES

- [1] Jacobs, M. J. N., Van Dingenen, J. L. J. "Ballistic protection mechanisms in personal armor", *Journal of Materials Science* 2001, 36, 3137 – 3142.
- [2] Prat, N., Miras, A., Rongieras, F., Voiglio, E., Sarron, J.-C., "Contemporary body armor: technical data, injuries, and limits", *European Journal of Trauma and Emergency Surgery* 2012, 38, 95–105.
- [3] Karahan, M., Kus, A., Eren R., "An investigation into ballistic performance and energy absorption capabilities of woven aramid fabrics", *International Journal of Impact Engineering* 2008, 35, 499-510.

- [4] Zivkovic, I. D., Perisic, P. I., Burzic Z. H., Uskokovic, P. S., Aleksic, R. R., "Aramid fiber reinforced laminar thermoplastic composite materials", *Journal of Advanced Materials* 2005, 37, 23-31.
- [5] Pinto, R., Carr, D., Helliker, M., Girvan, L., Gridley, N., "Degradation of military body armor due to wear: Laboratory testing", *Textile Research Journal* 2012, 82, 1157-1163.
- [6] Grujicic, M., Bell, W.C., Arakere, G., He, T., Xie, X., Cheeseman, B. A., "Development of a Meso-Scale Material Model for Ballistic Fabric and Its Use in Flexible-Armor Protection Systems", *Journal of Materials Engineering and Performance* 2010, 19, 22-39.
- [7] Mahfuz, H., Clements, F., Rangari, V., Dhanak, V., Beamsom, G., "Enhanced stab resistance of armor composites with functionalized silica nanoparticles", *Journal of Applied Physics* 2009, 105, 064307.
- [8] Toriki, A. M., Stojanović D. B., Živković I. D., Marinković, A., Škapin, S. D., Uskoković, P. S., Aleksić, R. R., "The viscoelastic properties of modified thermoplastic impregnated multi-axial aramid fabrics", *Polymer Composites* 2012, 33, 158-180.
- [9] Stojanovic, D., Orlovic, A., Glisic, S. B., Markovic, S., Radmilovic, V., Uskokovic, P. S., Aleksic, R., "Preparation of MEMO silane-coated SiO<sub>2</sub> nanoparticles under high pressure of carbon dioxide and ethanol", *The Journal of Supercritical Fluids* 2010, 52, 276-284.
- [10] Utracki, L. A., "In Rigid Ballistic Composites", NRC Publications Archive: Canada, 2010.
- [11] Decker, M. J., Halbach C. J., Nam C. H., Wagner, N. J., Wetzel E. D., "Stab resistance of shear thickening fluid (STF)-treated fabrics", *Composites Science and Technology* 2007, 67, 565-578.
- [12] Lee, Y. S., Wetzel, E. D., Wagner, N. J., "The ballistic impact characteristics of Kevlar® woven fabrics impregnated with a colloidal shear thickening fluid", *Journal of Materials Science* 2003, 38, 2825-2833.
- [13] Ballistic Resistance of Personal Body Armor, NIJ Standard – 0101.04, <https://www.ncjrs.gov/pdffiles1/nij/183651.pdf>.
- [14] Menard, K., *Dynamic Mechanical Analysis: A Practical Introduction*, 2nd Ed. CRC Press, Boca Raton, 2007.

**AUTHORS' ADDRESSES**

**Vera Obradović**

**Dušica B. Stojanović, PhD**

**Radmila Jančić – Heinemann, PhD**

**Irena Živković, PhD**

**Vesna Radojević, PhD**

**Petar S. Uskoković, PhD**

**Radoslav Aleksić, PhD**

University of Belgrade, Faculty of Technology and  
Metallurgy

Karnegijeva 4

Belgrade, Serbia 11120

SERBIA